Acta Pharmacologica Sinica (2013) 34: 129–136

www.nature.com/aps

Original Article

Voltage-gated K^+ channels in adipogenic differentiation of bone marrow-derived human mesenchymal stem cells

Mi-hyeon YOU[1], Min Seok SONG[2], Seul Ki LEE[2], Pan Dong RYU[2], So Yeong LEE[2, *], Dae-yong KIM[1, *]

Laboratory of [1]Veterinary Pathology and [2]Pharmacology, College of Veterinary Medicine and Research Institute for Veterinary Science, Seoul National University, Seoul, 151–742, Korea

Aim: To determine the presence of voltage-gated K^+ (Kv) channels in bone marrow-derived human mesenchymal stem cells (hMSCs) and their impact on differentiation of hMSCs into adipocytes.

Methods: For adipogenic differentiation, hMSCs were cultured in adipogenic medium for 22 d. The degrees of adipogenic differentiation were examined using Western blot, Oil Red O staining and Alamar assay. The expression levels of Kv channel subunits Kv1.1, Kv1.2, Kv1.3, Kv1.4, Kv2.1, Kv3.1, Kv3.3, Kv4.2, Kv4.3, and Kv9.3 in the cells were detected using RT-PCR and Western blot analysis.

Results: The expression levels of Kv2.1 and Kv3.3 subunits were markedly increased on d 16 and 22. In contrast, the expression levels of other Kv channel subunits, including Kv1.1, Kv1.2, Kv1.3, Kv1.4, Kv4.2, Kv4.3, and Kv9.3, were decreased as undifferentiated hMSCs differentiated into adipocytes. Addition of the Kv channel blocker tetraethylammonium (TEA, 10 mmol/L) into the adipogenic medium for 6 or 12 d caused a significant decrease, although not complete, in lipid droplet formation and adipocyte fatty acid-binding protein 2 (aP_2) expressions. Addition of the selective Kv2.1 channel blocker guangxitoxin (GxTX-1, 40 nmol/L) into the adipogenic medium for 21 d also suppressed adipogenic differentiation of the cells.

Conclusion: The results demonstrate that subsets of Kv channels including Kv2.1 and Kv3.3 may play an important role in the differentiation of hMSCs into adipocytes.

Keywords: human mesenchymal stem cells; adipogenic differentiation; voltage-gated K^+ channels; Kv2.1; Kv3.3; TEA; GxTX-1

Acta Pharmacologica Sinica (2013) 34: 129–136; doi: 10.1038/aps.2012.142; published online 10 Dec 2012

Introduction

Human mesenchymal stem cells (hMSCs) have attracted considerable research interest by virtue of their high proliferative capacity and potential for differentiating along multiple cellular lineages[1, 2]. With recent technical advances, hMSCs can be induced to differentiate *in vitro* and *in vivo* into specific cell types, such as osteocytes, adipocytes, and neurons[2–4]. A number of factors are critical for differentiation of hMSCs along a particular lineage, including cell density, mechanical forces, and multifactorial stimulation with specific nutrients[3–7]. For example, insulin, insulin-like growth factor I, glucocorticoids, and other growth hormones are known to be essential for adipogenic differentiation *in vitro*[2, 4, 7–9].

Voltage-gated K^+ (Kv) channels are important in maintaining cellular excitability in neurons and muscle cells. Recent reports also suggest that Kv channels participate in several other essential cell functions, such as proliferation, apoptosis, and migration[10–12]. To date, the activities of several ion channels, including delayed rectifier-like K^+, Ca^{2+}-activated K^+, transient outward K^+, and transient inward Na^+ channels, have been reported in hMSCs[13]. However, their expression patterns and roles during differentiation into cells of a specific lineage have not been well characterized[2, 13].

The present study was, therefore, designed to characterize the Kv channels related to adipogenic differentiation and to investigate their potential functions in bone marrow-derived human mesenchymal stem cells (hMSCs) during adipogenic differentiation.

Materials and methods

Cell culture and adipogenic differentiation

Cultured hMSCs, obtained originally from aspirates from the iliac crest of normal human donors, were purchased from

* To whom correspondence should be addressed.
E-mail daeyong@snu.ac.kr (Dae-yong KIM);
leeso@snu.ac.kr (So Yeong LEE)
Received 2012-01-20 Accepted 2012-09-18

FCB-Pharmicell Co, Ltd (Sungnam, South Korea). hMSCs isolation and culture procedures were performed according to South Korean GMP (good manufacturing practices). The hMSCs were maintained in growth medium (GM) consisting of low-glucose Dulbecco's modified Eagle's medium (DMEM) containing 10% fetal bovine serum (FBS), 0.3 mg/mL glutamine, 100 units/mL penicillin, and 100 μg/mL streptomycin at 37 °C in a humidified atmosphere of 95% air and 5% CO_2. Fifth-passage hMSCs were used in all experiments. For adipogenic differentiation, cells at passage 5 were harvested using trypsin/EDTA, plated in six-well plates at a concentration of 20 000 cells/cm^2 and incubated for 24 h to allow cell attachment. After reaching 100% confluence, cells were then transferred to adipogenic medium (AM) containing GM with 100 μmol/L *L*-ascorbate acid (Sigma-Aldrich, MO, USA), 1 μmol/L dexamethasone (Calbiochem, Germany), 0.5 mmol/L 3-isobutyl-1-methylxanthine (IBMX; Sigma-Aldrich), 100 μmol/L indomethacin (Sigma-Aldrich), and 10 μg/mL human recombinant insulin (Sigma-Aldrich) for 22 d[6, 13]. Cells in the control group were cultured in GM.

Reverse transcription-polymerase chain reaction

Total RNA was isolated using TRIzol reagent (Invitrogen, CA, USA) and was reverse transcribed by incubating at 25 °C for 5 min (annealing), 42 °C for 60 min (extension), and 70 °C for 15 min (inactivation) using an ImProm-II™ reverse transcription system kit (Promega, WI, USA). Polymerase chain reaction (PCR) was performed using 2 μL of cDNA, 16 μL of i-Star-Master Mix Solution (Intron, South Korea), and 0.4 μmol/L gene-specific primers for peroxisome proliferator-activated receptor-γ (PPARγ), lipoprotein lipase (LPL), adipocyte fatty acid binding protein 2 (aP_2), and glyceraldehyde 3-phosphate dehydrogenase (GAPDH) (Table 1). The cycling conditions consisted of an initial denaturation at 94 °C for 5 min, 35 cycles of denaturation at 94 °C for 40 s, annealing at 52.3–65 °C for 40 s, and extension at 72 °C for 1 min, followed by a final extension at 72 °C for 7 min (Table 1).

Table 1. Primers for RT-PCR.

Subtype	Primer sequence (Forward/Reverse)	Annealing (°C)
aP_2	5′-GGCGCACAGTCCAAAATACAAA-3′ 5′-CAGCCTGGGCAATATAGCAAGAC-3′	58.5
LPL	5′-TGTAGATTCGCCCAGTTTCAGC-3′ 5′-AAGTCAGAGCCAAAAGAAGCAGC-3′	57.7
PPARγ	5′-CCTATTGACCCAGAAAGCGATTC-3′ 5′-GCATTATGAGACATCCCCACTGC-3′	57.7
GAPDH	5′-ACCACAGTCCATGCCATCA-3′ 5′-TCCACCACCCTGTTGCTGT-3′	55.5

Western blot analysis

Cells plated on six-well plates were lysed in lysis buffer containing a protease inhibitor cocktail (CalBiochem), according to the manufacturer's instructions. The proteins were separated by sodium dodecyl sulfate-polyacrylamide gel electrophoresis (SDS-PAGE) and then transferred to polyvinylidene difluoride membranes (Bio-Rad, CA, USA). After blocking with 5% nonfat milk, membranes were incubated for 12 h at 4 °C with rabbit anti-aP_2 (Abcam, MA, USA), anti-Kv2.1 (Abcam), anti-Kv3.3 (Abcam) and anti-β-actin (Cell Signaling Technology, MA, USA) antibodies. Following incubation with donkey horseradish peroxidase-conjugated anti-rabbit secondary antibody (1:2000, GM Healthcare, NJ, USA), the samples were visualized using an enhanced chemiluminescent detection kit (Abfrontier, South Korea).

Real-time RT-PCR

cDNA was prepared by reverse transcription (RT) from total RNA isolated from cells grown in six-well plates, as described above. Diluted cDNA, 2× SYBR Green Master Mix (Applied Biosystems, CA, USA), and 0.4 μmol/L forward and reverse primers for Kv1.1, Kv1.2, Kv1.3, Kv1.4, Kv2.1, Kv3.1, Kv3.3, Kv4.2, Kv4.3, or Kv9.3 as in Table 2 were mixed. Quantitative RT-PCR was performed using an ABI Prism 7000 sequence detector (Applied Biosystems, CA, USA). The cycling conditions included an initial incubation at 50 °C for 2 min and 95 °C for 10 min, then 40 cycles of 95 °C for 15 s and 60 °C for 60 s. A dissociation protocol consisting of 95 °C for 15 s, 60 °C for 20 s, and 95 °C for 15 s was added to verify that the primer pair produced only a single product. Melting curves showed a single, sharp peak, indicating one PCR product. Relative mRNA target expression levels were calculated using the compara-

Table 2. Primers for real-time RT-PCR.

Subtype	Primer sequence (Forward/Reverse)	Annealing (°C)
Kv1.1	5′-TTACGAGTTGGGCGAGGA-3′ 5′-TGACGATGGAGATGAGGATG-3′	60
Kv1.2	5′-ATGAGAGAATTGGGCCTCCT-3′ 5′-CCCACTATCTTTCCCCCAAT-3′	60
Kv1.3	5′-TTCTCCTTCGAACTGCTGGT-3′ 5′-CTCAGGATGGCCAGAGACAT-3′	60
Kv1.4	5′-ACGAGGGCTTTGTGAGAGA-3′ 5′-TAAGATGACCAGGACGGACA-3′	60
Kv2.1	5′-GTTGGCCATTCTGCCTACT-3′ 5′-AGTGAAGCCCAGAGACTGGA-3′	60
Kv3.1	5′-GAGGACGAGCTGGAGATGAC-3′ 5′-AAGGTGGTGATGGAGACCAG3′	60
Kv3.3	5′-TGTGAGATGCCTGTGAGAGC-3′ 5′-GGAATCCGATGAGAACTCCA-3′	60
Kv4.2	5′-GCCTTCTTCTGCTTGGACAC-3′ 5′-TCATCACCAGCCCAATGTAA-3′	60
Kv4.3	5′-GTCTCCGCCTTGAAAACCA-3′ 5′-TCCAGGCACAAGTCTCAGTG-3′	60
Kv9.3	5′-CAGTGAGGATGCACCAGAGA-3′ 5′-TTGCTGTGCAATTCTCCAAG-3′	60
GAPDH	5′-GCAAGAGCACAAGAGGAAGA-3′ 5′-AAGGGGTCTACATGGCAACT-3′	60

tive cycle threshold (ddCt) method[14] and were normalized to those of GAPDH. Three independent experiments were performed in triplicate.

Cytotoxicity

The cytotoxicity of tetraethylammonium (TEA, Sigma Aldrich) was determined using MTT (3-[4,5-dimethylthiazol-2-yl]-2,5-diphenyltetrazolium bromide) assays (Amresco, OH, USA). The hMSCs were seeded into 96-well plates (20 000 cells/well) and, after growing for 12 h in AM containing 20% FBS, were serum-starved by culturing for 24 h in AM containing 2% FBS. Cells were then switched to 20% FBS supplemented with 10 mmol/L TEA for 24 h. MTT assays were performed as previously described[15]. Untreated cells were used as controls. All samples (n=3 for each condition) were run in triplicate in each experiment.

The cytotoxicity of TEA and guangxitoxin (GxTX-1; Bioscience Export, Japan) was also determined by Alamar Blue reduction. For these assays, 10×Alamar Blue solution (Biosource, CA, USA) was added to each culture well, and the plates were incubated at 37 °C for 2 h. Plates were then read at dual wavelengths of 540 and 630 nm on a microplate reader. A 1% Triton X-100 solution, which causes 100% cytotoxicity, was used as a negative control and hMSCs cultured in GM were used as a positive control. Percent cytotoxicity was calculated using the following equation: Cytotoxicity (%)=(experimental value – untreated control)/(positive control – untreated control)×100[16]. All samples (n=3 each) were run in triplicate in each experiment.

Oil Red O staining

Cells were stained with Oil Red O as previously described[2]. Briefly, cells were fixed in a 10% solution of formaldehyde in aqueous phosphate buffer for about 1 h. After washing with 60% isopropanol, cells were stained with Oil red O solution (in 60% isopropanol) for 10 min, washed repeatedly with water, and destained in 100% isopropanol for 15 min. The optical density of the solution at 500 nm (OD_{500}) was measured.

Electrophysiological recordings

The prepared hMSCs were transferred to the recording chamber and allowed to attach to the bottom of the chamber for 20 min. The cells were visualized by the differential interference contrast video microscopy. Patch pipettes were pulled from the borosilicate glass capillaries (1.7 mm diameter; 0.5 mm wall thickness), resulting in an open resistance ranging from 3 to 6 MΩ. The recording solutions were prepared as previously described[17]: the pipette internal solution (in mmol/L) contained 150 KCl, 1 $MgCl_2$, 10 HEPES, 5 EGTA, and 2 Mg-ATP (the pH was adjusted to 7.2 with KOH); the bath solution (in mmol/L) contained 143 NaCl, 5.4 KCl, 0.5 $MgCl_2$, 1.8 $CaCl_2$, 0.5 NaH_2PO_4, 10 glucose, and 5 HEPES (the pH was adjusted to 7.4 with NaOH). Electrical signals were recorded in the whole cell configuration using the Axoclamp 2B amplifier (Axon Instruments, Foster City, CA, USA). The signals were filtered at 1 kHz and digitized at 10 kHz using an analog-digital converter (Digidata 1320A, Axon Instruments) and pClamp software (Version 9.0, Axon Instruments). The membrane potentials were measured in the current-clamp mode.

Statistical analysis

All data are presented as the standard error of the mean (SEM). Unpaired Student's t-tests were used for analysis of real-time RT-PCR and MTT assay data. One-way ANOVA test were used for analysis of membrane potential measurement. Differences between mean values with P-values <0.05 were considered significant. GraphPad Prism version 4.0 (CA, USA) and Origin version 8 (MA, USA) was used for the statistical analyses.

Results

Adipogenic differentiation of hMSCs

To induce adipocyte differentiation, we cultured hMSCs (passage 5) in six-well plates with AM, and analyzed the time course of morphological change and expression of marker proteins. The cells began to exhibit small-sized lipid droplets in their cytoplasm on d 3 of AM treatment. On d 8, Oil Red O staining revealed marked increases (about 50%) in cytoplasmic lipid droplets (Figure 1A). By d 22, approximately 80% to 90% of the hMSCs cultured in AM were mature human adipocytes containing large monocular lipid droplets (Figure 1A). No lipid droplets were observed on d 8, 16, or 22 in cells cultured in GM (Figure 1A). A quantitative spectrophotometric analysis of Oil Red O stained cells eluted with isopropanol showed that hMSCs cultured in AM exhibited a progressive increase in OD_{500} compared to cells in the control group (P<0.001; Figure 1A). Moreover, mRNA expression of the adipogenesis markers, PPARγ, LPL, and aP_2, was detectable in AM-cultured hMSCs from d 8 (Figure 1B). The protein expression of aP_2, the main component of the intracellular fatty acid-binding protein family which is regarded as a marker of terminal cell differentiation[18, 19], markedly increased during differentiation (Figure 1C). aP_2 is known as an important mediator of intracellular transport and the metabolism of fatty acids, and its expression during adipogenic differentiation is regulated through PPARγ and CCAAT/enhancer-binding protein α (C/EBPα)[18]. We also conducted RT-PCR for both osteogenic (osteopontin, osteocalcin) and chondrogenic (Type II collagen) makers to confirm the lineage specificity of differentiation. No differentiation into either osteogenic or chondrogenic lineages was detected (data not shown), thus confirming that hMSCs cultured with AM differentiated only into adipogenic-lineage cells in a controlled manner.

mRNA and protein (Kv2.1 and Kv3.3) expression of Kv channels in hMSCs during adipogenesis

To explore the expression patterns of various Kv channels in hMSCs during adipogenic differentiation, we conducted real-time quantitative RT-PCR on d 0 (undifferentiated), 8, 16, and 22 of AM differentiation. The only Kv channel subtypes that showed a correlation between mRNA expression and adipogenic differentiation of hMSCs were Kv2.1 and Kv3.3, which

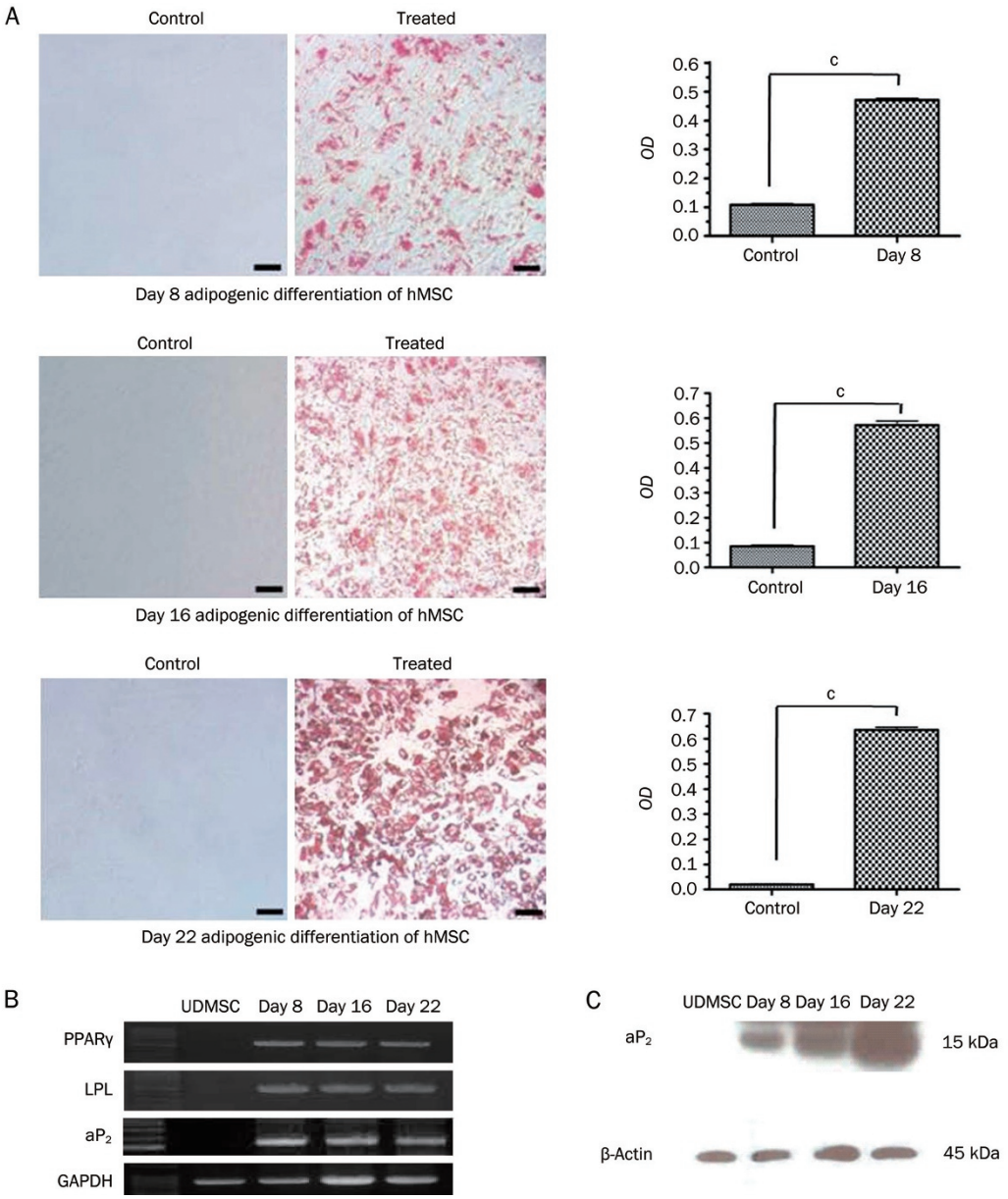

Figure 1. Phenotypical characterization during adipogenic differentiation of hMSCs. (A) Differentiation of hMSCs into adipocytes was confirmed by Oil Red O staining 8, 16, and 22 d after inducing adipogenic differentiation (n=3). Microscopic images of hMSCs were taken (scale bar=100 μm). Compared to hMSCs cultured with GM, hMSCs cultured with AM exhibited significantly increased OD_{500} levels in quantitative Oil Red O staining ($^cP<0.001$). (B) RT-PCR analysis for the adipogenic markers, PPARγ, LPL, and aP_2 (n=3). (C) Western blot analysis for aP_2 using undifferentiated hMSCs and adipogenic-differentiated hMSCs on d 8, 16, and 22 (n=3). Molecular sizes are given in kDa. β-Actin was used as a control for equal loading.

showed a significant increase in mRNA levels on d 16 and 22 compared to d 8 (Figure 2A). In contrast, the expression levels of other Kv channels, including Kv1.1, Kv1.2, Kv1.3, Kv1.4, Kv4.2, Kv4.3, and Kv9.3, decreased as undifferentiated hMSCs differentiated into adipocytes. The expression pattern of Kv3.1 differed from that of the other Kv channels; its expression was significantly increased on d 8, and then decreased on d 16 and 22 (Figure 2B).

The protein expression levels were measured using Western blot analysis for Kv2.1 and Kv3.3, which demonstrated a significant increase in protein levels during adipogenic differentiation (Figure 3). As shown in Figure 3A, the protein expression level of Kv2.1 was increased on d 21. The protein expression level of Kv3.3 was not detected on d 16 (Figure 3B), which does not correlate with the real-time RT-PCR analysis. This discrepancy could be due to post-transcriptional, translational, or post-translational regulation as suggested by Chen *et al*[20] .

Measurement of membrane potential on adipogenic differentiation of hMSCs

The membrane potentials of the hMSCs were measured dur-

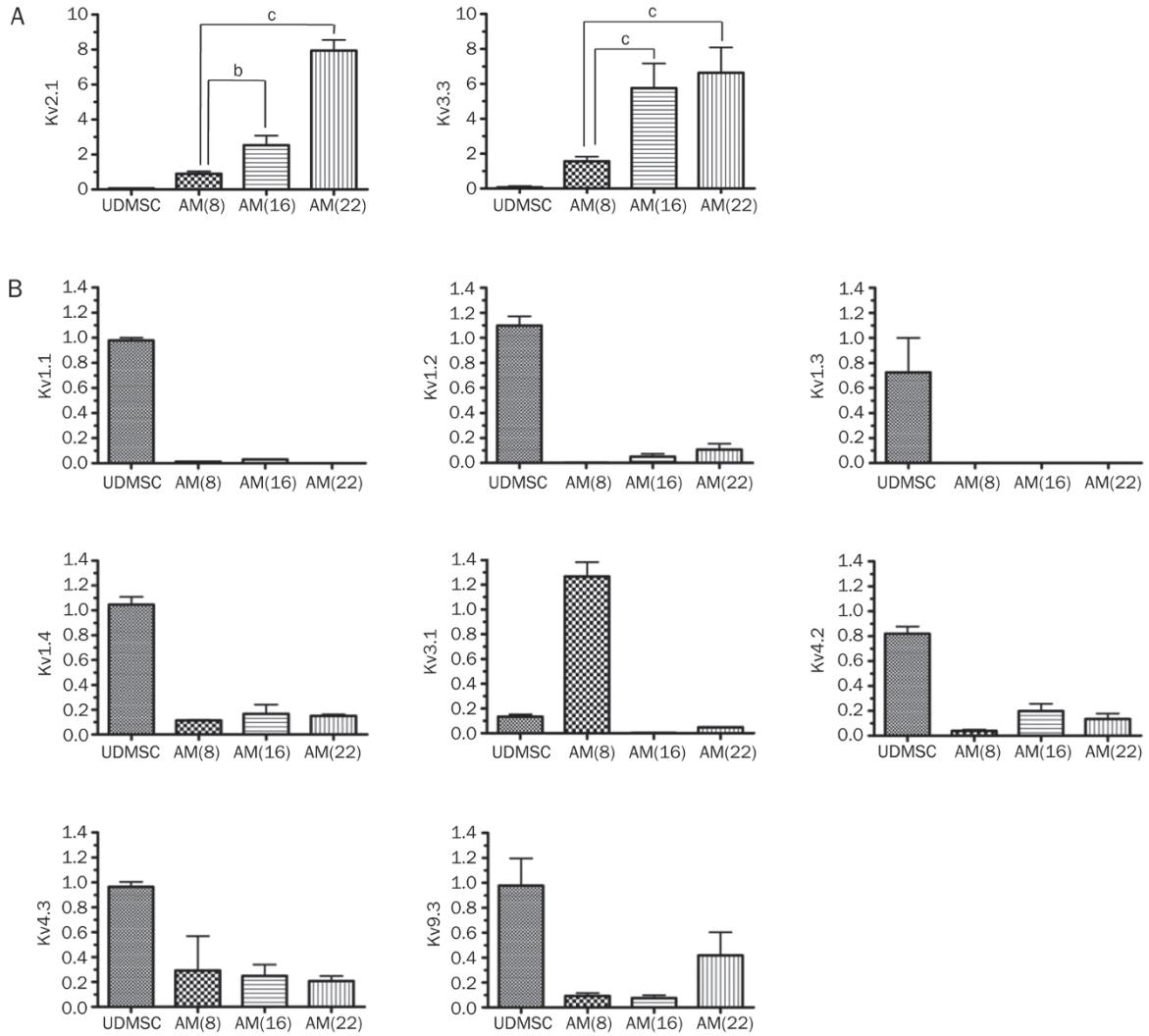

Figure 2. Expression of Kv channel mRNAs during adipogenic differentiation of hMSCs. (A) Quantification of Kv2.1 and Kv3.3 mRNA expression by real-time RT-PCR. Kv2.1 mRNA levels in hMSCs on d 16 and 22 after inducing adipogenic differentiation were significantly increased compared to those on d 8 ($^{b}P<0.05$; $^{c}P<0.01$) (n=3). (B) Quantification of Kv channel mRNA levels by real-time RT-PCR. Data points represent mean±SEM (n=3).

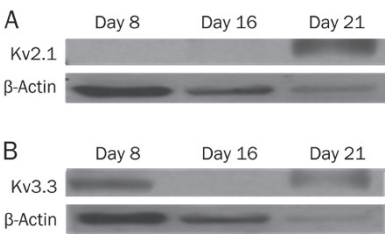

Figure 3. Western blot analysis of (A) Kv2.1 and (B) Kv3.3. The protein expression level of Kv2.1 was increased during adipogenic differentiation (n=2). The protein expression level of Kv3.3 was not detected on d 16 (n=2).

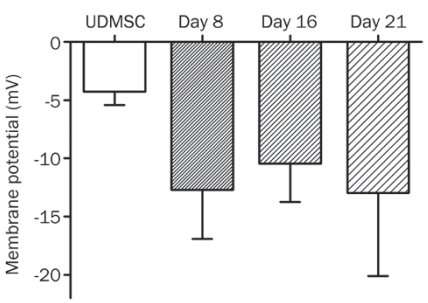

Figure 4. Membrane potential measurement during adipogenic differentiation of hMSCs. The membrane potentials of undifferentiated MSC (UDMSC) and differentiated MSCs were recorded using a whole cell current-clamp technique. Compared to the UDMSC (n=8), the MSCs in progress of differentiation (d 8, n=12; d 16, n=7) or differentiated (d 21, n=7) displayed the more hyperpolarized membrane potential. However, there was no statistical difference among the groups (the one-way ANOVA test).

ing adipogenic differentiation of the hMSCs. As shown in Figure 4, the membrane potential on d 0 was -4.28±1.15 mV (n=8), and the membrane potential on d 8, 16, and 22 of AM differentiation was -12.72±4.20 (n=12), -10.46±3.30 (n=7), and

-12.98±7.13 mV (n=7), respectively. The differentiated cells showed more hyperpolarized membrane potentials compared to the undifferentiated cells. However, there was no statistical difference among the groups.

Effect of TEA and GxTX-1 on adipogenic differentiation of hMSCs

Next, we investigated the function of Kv channels in hMSCs during adipogenic differentiation. In order to test whether Kv channels play a role in adipogenic differentiation, we blocked these channels using the nonselective K^+ channel blocker, TEA[15]. First, we conducted MTT assays to determine if blocking Kv channels using TEA affected cell viability. MTT assays showed that cell viability was not significantly different following a 24 h treatment of cells with 10 mmol/L TEA, a concentration known to effectively block Kv channels[15]. We also tested the effects of TEA treatments of longer duration, performing MTT assays on cells incubated with 10 mmol/L TEA for 1, 3, 6, 9, and 12 d. In each of these time periods, TEA significantly decreased cell viability; these effects were compensated for the following experiments.

To investigate the effects of Kv channels on the adipogenic differentiation of hMSCs, we exposed hMSCs to TEA during adipogenic differentiation, pretreating cells with TEA for 1 d before inducing adipogenic differentiation, and continuing for 6 or 12 d, as shown in Figure 5A. After culturing to d 21, lipid droplet morphology and aP_2 protein expression levels were analyzed. Treatment with TEA for either 6 or 12 d significantly inhibited large lipid droplet formation compared to cells in the untreated (AM only) control group, as evidenced by a decrease in the OD_{500} values obtained in quantitative Oil Red O staining experiments (Figure 5B). In addition, expression of the adipocyte marker aP_2 was significantly decreased in TEA-treated groups (Figure 5B)[18]. No lipid droplets were observed in cells cultured in the negative control medium (GM). These results indicate that blocking Kv channel function inhibits adipogenic differentiation of hMSCs.

Our real-time RT-PCR and Western analysis revealed that Kv2.1 channel expression was significantly up-regulated during adipogenic differentiation. In order to determine if Kv2.1 channels are involved in regulating adipogenic differentiation, we used the selective Kv2.1 channel blocker, GxTX-1[21, 22]. As shown in Figure 5C, Oil Red O staining was significantly decreased following treatment with 40 nmol/L GxTX-1, a concentration known to effectively block Kv2.1 channels[21] for 21 d; however, the extent of inhibition was less than that imposed by TEA. These results suggest that, although Kv2.1 is among the Kv channels involved in adipogenic differentiation, several Kv channels likely collaboratively contribute to the differentiation of hMSCs. A likely candidate channel is Kv3.3, which also showed a significant increase in mRNA expression during adipogenic differentiation. However, at present, no Kv3.3-specific blockers are commercially available. Thus, assessing the effects of Kv3.3 on adipogenic differentiation will have to await the future development of selective pharmacological agents.

Discussion

In the present study, we investigated the roles of Kv channels in the adipogenic differentiation of hMSCs. Based on our study, certain Kv channels including Kv2.1 are involved in the adipogenic differentiation of hMSCs since specific blockade of the Kv channels decreased the extent of adipogenic differentiation of the hMSCs. The role of Kv2.1 on adipogenic differentiation has not been previously reported. The expression of Kv2.1 in MSCs was previously reported in rat/rabbit bone marrow and mouse neural progenitor cells[23–25]; however, neither their expression patterns nor their roles during adipogenesis were known at the present time.

The roles of Kv channels during the adipogenic differentiation of hMSCs have not been previously reported. However, several Kv channels have been identified in undifferentiated cells, and the degree of expression of several Kv channels, namely Kv1.1, Kv1.7, Kv2.1, Kv2.2, and Kv3.1, has been reported to increase considerably during the differentiation process in neural progenitor cells[25]. Based on our data, the mRNA expression of Kv1.1 was decreased and the expression of Kv3.1 was different depending on the stage of adipogenic differentiation, which differs from the previous report[25]. The discrepancy may be due to differences in cell types, and further studies are necessary to determine the activities of specific Kv channels in different cells.

It has been demonstrated that Kv channels regulate skeletal muscle differentiation and that modulation of Kv7 using Kv channel activator also has an effect on skeletal muscle differentiation[26]. In addition, TEA has been shown to inhibit the differentiation of white adipose cells from preadipocytes, suggesting the involvement of Kv channels in adipogenesis in these cells, although specific K^+ channel subtypes were not defined[9]. Therefore, expression of Kv channels in undifferentiated cells and alterations in Kv channels during differentiation may somehow be involved in the differentiation process.

In addition to Kv channels, the activity of other ion channels, such as the voltage-gated Ca^{2+} channel, is also reported to correlate with cellular differentiation[27]. For example, blockade of Ca^{2+} entry through L-type Ca^{2+} channels inhibits switching to the neuronal lineage in neural progenitor cells, suggesting an important role for these channels in regulating neuronal differentiation[27].

The mechanisms by which ion channels contribute to the regulation of cellular differentiation are not clearly understood. To date, it has been reported that the hyperpolarization of membrane potential in undifferentiated hMSCs could induce adipogenic and osteogenic differentiation after 4 weeks, suggesting that ion channels may play a role in controlling these cellular processes[2]. However, a bioelectric signaling mechanism does not completely explain the role of ion channels, and ion-independent ion channel signaling is also proposed[28]. According to our study, the membrane potential was not significantly altered during adipogenic differentiation. Therefore, membrane potential could not be the sole mechanism to explain the involvement of Kv channels in adipogenic

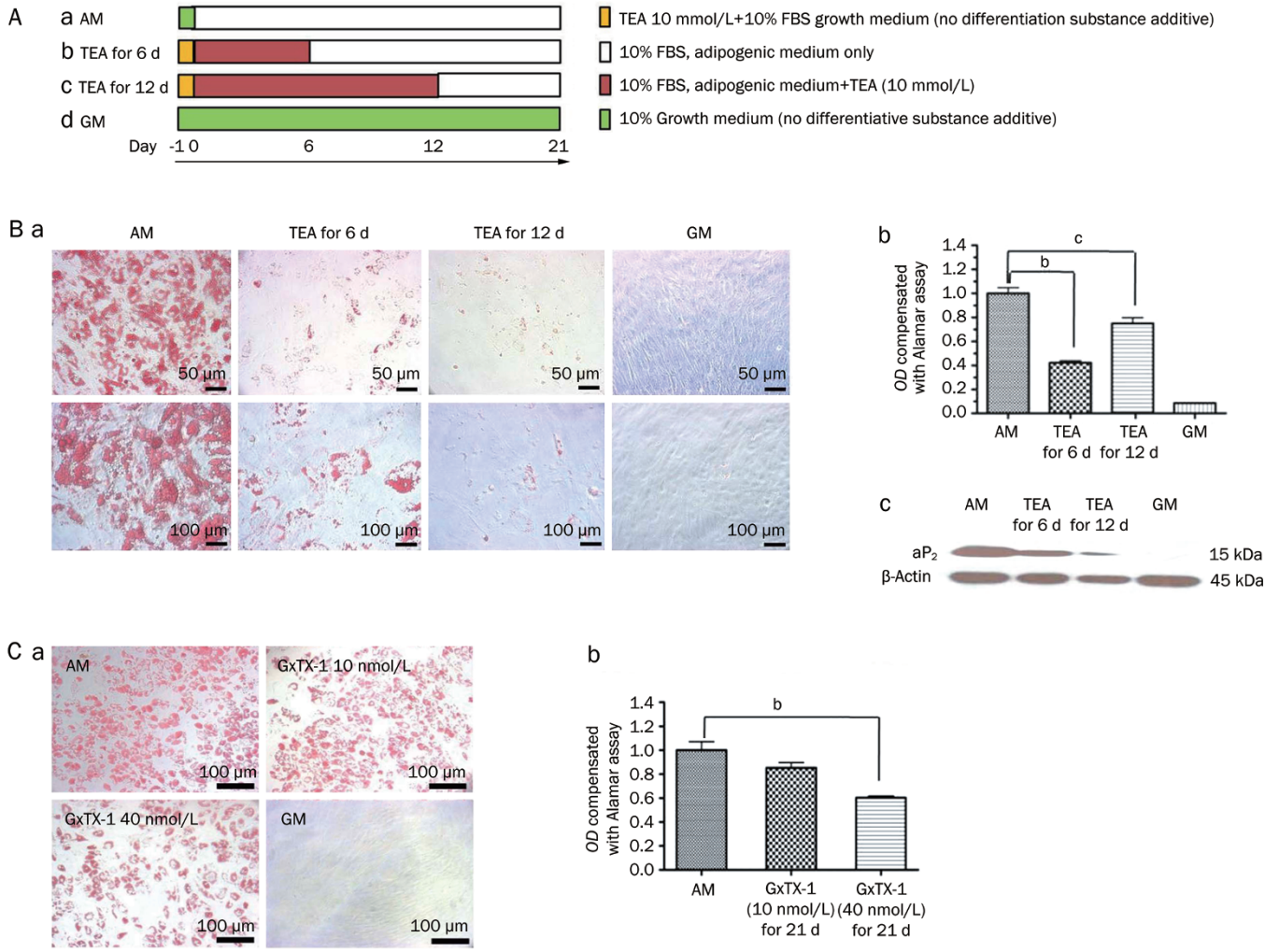

Figure 5. Role of Kv channel function during adipogenic differentiation of hMSCs. (A) Protocol for TEA treatment during the adipogenic differentiation of hMSCs. Cells were pretreated with 10 mmol/L TEA for 1 d before inducing differentiation, and then were maintained in TEA until 6 d (b) or 12 d (c) after differentiation (n=3). Group (a) is a positive control group treated with AM, and group (d) is a negative control group treated with GM. (B) Effect of TEA on adipogenic differentiation of hMSCs. (a) Differentiation of hMSCs into adipocytes was confirmed on d 21 by Oil Red O staining. Microscopic images were taken (lower-image scale bar=100 μm; higher-image scale bar=50 μm) (b) Graph of Alamar assay-compensated, quantitative Oil Red O-staining data (OD_{500}). Data points represent mean±SEM (n=3). OD_{500} levels for 6- and 12-d TEA-treated groups were significantly decreased compared to the AM group (^bP<0.05; ^cP<0.01). (c) Western blot analysis of aP_2 protein expression (n=3). Molecular sizes are given in kDa. β-Actin was used as a control for equal loading. (C) Effect of GxTX-1 on adipogenic differentiation of hMSCs. (a) Differentiation of hMSCs into adipocytes was confirmed on d 21 by Oil Red O staining. Microscopic images were taken (image scale bars=100 μm). AM, treated positive control; GM, treated negative control. GM-cultured hMSCs were treated with 10 or 40 nmol/L GxTX-1 for 21 d. (b) Graph of Alamar assay-compensated, quantitative Oil Red O-staining data (OD_{500}). Data points represent mean±SEM (n=3). OD_{500} levels in GxTX-1 (40 nmol/L)-treated groups were significantly decreased on d 21 compared to those in hMSCs cultured with AM only (^bP<0.05).

differentiation. Future studies are warranted to identify the specific mechanisms in this process.

Taken together, our data demonstrate the alterations of Kv channel expression during adipogenic differentiation of hMSCs. Kv2.1 expression was significantly increased at 22 d. We found that blocking the Kv channels with TEA significantly decreased, although not completely, lipid droplet formation (demonstrated by the quantitative and qualitative analysis of Oil Red O staining) and aP_2 expression levels—effects that were dependent upon the duration of TEA treatment. Moreover, selective inhibition of Kv2.1 channels using GxTX-1 suppressed adipogenic differentiation. These results suggest that Kv channels, including Kv2.1, may be involved in the adipogenic differentiation of hMSCs. These results further imply that modulation of Kv channels might be applicable in pathological conditions associated with excessive marrow adipogenesis and warrants further investigation on the mechanisms involved.

Acknowledgements

This research was supported by the Basic Science Research Program through the National Research Foundation of Korea (NRF) funded by the Ministry of Education, Science and Technology (2011-0014514).

Author contribution

Mi-hyeon YOU performed experiments and analyzed the data; Min Seok SONG performed Western blot analysis for Kv2.1 and Kv3.3; Seul Ki LEE and Pan Dong RYU performed the electrophysiological recording; So Yeong LEE designed research, interpreted the data and drafted the article; and Daeyong KIM designed research, interpreted the data and drafted the article.

References

1 Serakinci N, Keith WN. Therapeutic potential of adult stem cells. Eur J Cancer 2006; 42: 1243–6.
2 Sundelacruz S, Levin M, Kaplan DL. Membrane potential controls adipogenic and osteogenic differentiation of mesenchymal stem cells. PLoS One 2008; 3: e3737.
3 Yu YL, Chou RH, Chen LT, Shyu WC, Hsieh SC, Wu CS, *et al*. EZH2 regulates neuronal differentiation of mesenchymal stem cells through PIP5K1C-dependent calcium signaling. J Biol Chem 2011; 286: 9657–67.
4 Hebert TL, Wu X, Yu G, Goh BC, Halvorsen YD, Wang Z, *et al*. Culture effects of epidermal growth factor (EGF) and basic fibroblast growth factor (bFGF) on cryopreserved human adipose-derived stromal/stem cell proliferation and adipogenesis. J Tissue Eng Regen Med 2009; 3: 553–61.
5 Park JS, Yang HN, Woo DG, Jeon SY, Do HJ, Lim HY, *et al*. Chondrogenesis of human mesenchymal stem cells mediated by the combination of SOX trio SOX5, 6, and 9 genes complexed with PEI-modified PLGA nanoparticles. Biomaterials 2011; 32: 3679–88.
6 McBeath R, Pirone DM, Nelson CM, Bhadriraju K, Chen CS. Cell shape, cytoskeletal tension, and RhoA regulate stem cell lineage commitment. Dev Cell 2004; 6: 483–95.
7 Mur C, Arribas M, Benito M, Valverde AM. Essential role of insulin-like growth factor I receptor in insulin-induced fetal brown adipocyte differentiation. Endocrinology 2003; 144: 581–93.
8 Campbell JE, Peckett AJ, D'Souza AM, Hawke TJ, Riddell MC. Adipogenic and lipolytic effects of chronic glucocorticoid exposure. Am J Physiol Cell Physiol 2011; 300: C198–209.
9 Ramirez-Ponce MP, Mateos JC, Bellido JA. Insulin increases the density of potassium channels in white adipocytes: possible role in adipogenesis. J Endocrinol 2002; 174: 299–307.
10 O'Grady SM, Lee SY. Chloride and potassium channel function in alveolar epithelial cells. Am J Physiol Lung Cell Mol Physiol 2003; 284: L689–700.
11 O'Grady SM, Lee SY. Molecular diversity and function of voltage-gated (Kv) potassium channels in epithelial cells. Int J Biochem Cell Biol 2005; 37: 1578–94.
12 Warth R. Potassium channels in epithelial transport. Pflugers Arch 2003; 446: 505–13.
13 Bai X, Ma J, Pan Z, Song YH, Freyberg S, Yan Y, *et al*. Electrophysiological properties of human adipose tissue-derived stem cells. Am J Physiol Cell Physiol 2007; 293: C1539–50.
14 You MH, Kwak MK, Kim DH, Kim K, Levchenko A, Kim DY, *et al*. Synergistically enhanced osteogenic differentiation of human mesenchymal stem cells by culture on nanostructured surfaces with induction media. Biomacromolecules 2010; 11: 1856–62.
15 Schaarschmidt G, Wegner F, Schwarz SC, Schmidt H, Schwarz J. Characterization of voltage-gated potassium channels in human neural progenitor cells. PLoS One 2009; 4: e6168.
16 Kim S, Choi JE, Choi J, Chung KH, Park K, Yi J, *et al*. Oxidative stress-dependent toxicity of silver nanoparticles in human hepatoma cells. Toxicol *In Vitro* 2009; 23: 1076–84.
17 Park KS, Jung KH, Kim SH, Kim KS, Choi MR, Kim Y, *et al*. Functional expression of ion channels in mesenchymal stem cells derived from umbilical cord vein. Stem Cells 2007; 25: 2044–52.
18 Prawitt J, Niemeier A, Kassem M, Beisiegel U, Heeren J. Characterization of lipid metabolism in insulin-sensitive adipocytes differentiated from immortalized human mesenchymal stem cells. Exp Cell Res 2008; 314: 814–24.
19 Sun L, Nicholson AC, Hajjar DP, Gotto AM Jr, Han J. Adipogenic differentiating agents regulate expression of fatty acid binding protein and CD36 in the J744 macrophage cell line. J Lipid Res 2003; 44: 1877–86.
20 Chen G, Gharib TG, Huang CC, Taylor JM, Misek DE, Kardia SL, *et al*. Discordant protein and mRNA expression in lung adenocarcinomas. Mol Cell Proteomics 2002; 1: 304–13.
21 Herrington J. Gating modifier peptides as probes of pancreatic beta-cell physiology. Toxicon 2007; 49: 231–8.
22 Clement H, Odell G, Zamudio FZ, Redaelli E, Wanke E, Alagon A, *et al*. Isolation and characterization of a novel toxin from the venom of the spider *Grammostola rosea* that blocks sodium channels. Toxicon 2007; 50: 65–74.
23 Li GR, Deng XL, Sun H, Chung SS, Tse HF, Lau CP. Ion channels in mesenchymal stem cells from rat bone marrow. Stem Cells 2006; 24: 1519–28.
24 Deng XL, Sun HY, Lau CP, Li GR. Properties of ion channels in rabbit mesenchymal stem cells from bone marrow. Biochem Biophys Res Commun 2006; 348: 301–9.
25 Schaarschmidt G, Wegner F, Schwarz SC, Schmidt H, Schwarz J. Characterizatin of voltage-gated potassium channels in human neural progenital cells. PLoS One 2009; 4: e6168.
26 Iannotti FA, Panza E, Barrese V, Viggiano D, Soldovieri MV, Taglialatela M. Expression, localization, and pharmacological role of Kv7 potassium channels in skeletal muscle proliferation, differentiation, and survival after myotoxic insults. J Pharmacol Exp Ther 2010; 332: 811–20.
27 D'Ascenzo M, Piacentini R, Casalbore P, Budoni M, Pallini R, Azzena GB, *et al*. Role of L-type Ca^{2+} channels in neural stem/progenitor cell differentiation. Eur J Neurosci 2006; 23: 935–44.
28 Hegle AP, Marble DD, Wilson GF. A voltage-driven switch for ion-independent signaling by ether-a-go-go K^+ channels. Proc Natl Acad Sci U S A 2006; 103: 2886–91.